been made of the polarization parameter P for backward $\pi^+ p$ elastic scattering at incident momenta below 3.75 GeV/c.[14] The polarization shows significant variation over the momentum interval studied.

Since, at 6-GeV/c incident momentum, the relative phase between the f_{1s} and f_{3s} amplitudes remains constant over the region $-0.8<u<0$ (GeV/c)^2, it follows that any difference in phase between the nonflip and flip components of the amplitudes must be the same for both the f_{1s} and f_{3s} amplitudes. It also follows that any change in the phase of the f_{1s} amplitude produced by a change in the relative magnitudes of the two helicity components of f_{1s} must be exactly followed by a corresponding change in the phase of the f_{3s} amplitude. Thus, the polarization in all backward pion-nucleon processes at 6-GeV/c incident momentum must be similar in both magnitude and sign.

[14] R. Miller and A. Yokosawa, Argonne National Laboratory Report No. ANL/HEP 7001, 1970 (unpublished).

ACKNOWLEDGMENTS

We wish to extend our thanks to the entire ZGS staff for their kind cooperation and assistance toward the successful completion of the experiment, and also to our able staff of scanners under the leadership of Jerry Wright. We have had the advantage of a great many discussions with our theoretical colleagues at the University of Minnesota.

PHYSICAL REVIEW D VOLUME 2, NUMBER 11 1 DECEMBER 1970

Kaon-Nucleon Total Cross Sections from 0.36 to 0.72 GeV/c*

T. Bowen, P. K. Caldwell,† F. Ned Dikmen, E. W. Jenkins, R. M. Kalbach, D. V. Petersen, and A. E. Pifer

Department of Physics, University of Arizona, Tucson, Arizona 85721

(Received 16 July 1970)

The K^+ and K^- total cross sections were measured on both hydrogen and deuterium at a series of momenta between 360 MeV/c and 720 MeV/c by the transmission method. The data were corrected for Coulomb and decay effects, and the isospin states were extracted. The K^+N, $I=1$ cross section was found to be free from resonances, although the presence of a small dip at about 700 MeV/c was confirmed. No convincing evidence was found for structure in the K^+N, $I=0$ cross section, which was observed to be steeply rising with increasing momentum throughout this range. The prominence of the $\Lambda'(1520)$ was verified in the K^-N, $I=0$ system in which no additional structure was seen. In the K^-N, $I=1$ system no new structure was clearly established, though there appears to be a small enhancement with a mass about 1600 MeV.

I. INTRODUCTION

In recent years, very accurate measurements have been made on the $K^\pm$-nucleon total cross sections above a laboratory momentum of 1000 MeV/c.[1–4] The experiment by Bugg *et al.*[4] measured these cross sections above 600 MeV/c with typical errors of ± 0.2 mb. However, below 700 MeV/c their errors vary between ± 0.4 and ± 1.9 mb. Below 600 MeV/c,[5,6] previous measurements have errors of 2–3 mb, except for a recent K^-p bubble-chamber experiment[7] with errors of ± 1 mb, and no accurate judgment of the detailed behavior of the total cross section could be made.

It was decided to measure the total cross sections of charged kaons on hydrogen and deuterium to a statistical accuracy of about 1% in the region 350–720 MeV/c. This precision was judged necessary in order to reevaluate the S-wave scattering and effective-range parameters at very low energies. In addition it was thought possible that one or more yet undetected kaon-nucleon resonant structures might exist in the mass range 1500–1660 MeV. Only the $\Lambda'(1520)$ had previously been seen in the K^-p total cross section[6] and no structure at all had been detected in the K^+p total cross section.

* Work supported in part by a grant from the National Science Foundation.

† Present address: Physics Department, University of Michigan, Ann Arbor, Mich. 48104.

[1] R. L. Cool, G. Giacomelli, T. F. Kycia, B. A. Leontić, K. K. Li, A. Lundby, and J. Teiger, Phys. Rev. Letters **16**, 1228 (1966).

[2] R. L. Cool, G. Giacomelli, T. F. Kycia, B. A. Leontić, K. K. Li, A. Lundby, and J. Teiger, Phys. Rev. Letters **17**, 102 (1966).

[3] R. J. Abrams, R. L. Cool, G. Giacomelli, T. F. Kycia, B. A. Leontić, K. K. Li, and D. N. Michael, Phys. Rev. Letters **19**, 678 (1967).

[4] D. V. Bugg, R. S. Gilmore, K. M. Knight, D. C. Salter, G. H. Stafford, E. J. N. Wilson, J. D. Davies, J. D. Dowell, P. M. Hattersley, R. J. Homer, A. W. O'Dell, A. A. Carter, R. J. Tapper, and K. F. Riley, Phys. Rev. **168**, 1466 (1968).

[5] S. Goldhaber, W. Chinowsky, G. Goldhaber, W. Lee, T. A. O'Halloran, and T. F. Stubbs, Phys. Rev. Letters **9**, 135 (1962).

[6] M. B. Watson, M. Ferro-Luzzi, and R. D. Tripp, Phys. Rev. **131**, 2248 (1963).

[7] R. Armenteros, P. Baillon, C. Bricman, M. Ferro-Luzzi, E. Pagiola, J. O. Petersen, D. E. Plane, N. Schmitz, E. Burkhardt, N. Filthuth, E. Kluge, H. Oberlack. R. R. Ross, R. Barloutaud, P. Granet, J. Meyer, J. P. Porte, and J. Prevost, CERN Report No. D. Ph. II/PHYS. 70-7 (unpublished).

Because of the high statistical accuracy required, a counter technique was chosen for the cross-section measurements of the present experiment. This involves the use of a set of counters which subtend various solid angles at a target. The amount of incident beam transmitted through the target is then simultaneously measured with each counter. Comparison of the results of using full and empty targets permits correction for many of the effects not due to scattering by the target material. It is then possible to obtain a cross section for each counter to which corrections may be applied for effects other than scattering due to the strong interaction. These considerations will be discussed in detail in Sec. III, particularly those effects which are especially significant at very low momentum. The resulting cross sections then can be extrapolated to zero solid angle for a measurement of the total cross section.

II. APPARATUS

This experiment was conducted at the Lawrence Radiation Laboratory Bevatron with experimental apparatus designed to yield useful data for incident beam momenta from 300 to 800 MeV/c. Because of magnet limitations, the beam transport system was capable of producing momenta no higher then about 760 MeV/c, whereas the channel length prohibited usable flux below about 350 MeV/c.

A diagram of the beam layout and counters is shown in Fig. 1. The beam included a 10-ft electrostatic separator and a mass-momentum aperture at an intermediate focus. A kaon/pion ratio of 1/20 at 566 MeV/c for a positively charged beam and 1/150 for a negatively charged beam was available at the position of the hydrogen or deuterium target. Figure 2 shows the momentum distribution at the end of the beam channel generated by a Monte Carlo technique. The average momentum is 0.5% below the central momentum with a spread of $\pm 2.5\%$.

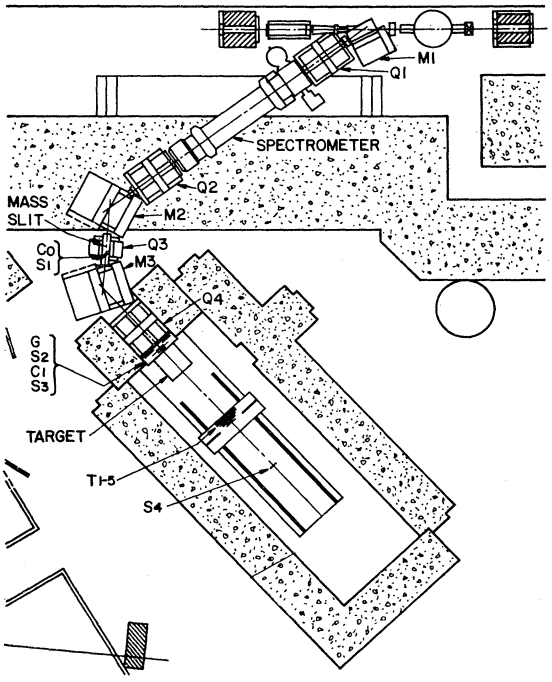

FIG. 1. Beam and counter layout.

The target was provided by the Lawrence Radiation Laboratory and consisted of three identical 6-in.-diam by 18-in.-long cylindrical flasks mounted in a common vacuum jacket. The downstream portion of the vacuum jacket was flared so as to reduce the effects of particles striking the aluminum walls. The hydrogen and deuterium flasks were continuously fed from reservoirs mounted over the targets. The hydrogen target was boiling slowly at atmospheric pressure while the deuterium target was isolated and in temperature equilibrium with the hydrogen target. The targets contained a small amount of catalyst so that they contained equilibrium concentrations of parahydrogen and orthodeuterium. The densities used were 0.0706 ± 0.0002 g/cm^3 for hydrogen and 0.1687 ± 0.0004 g/cm^3 for deuterium. The effective target length, 44.62 ± 0.03 cm, was determined by a consideration of the physical dimensions of the flask and the measured beam profile.

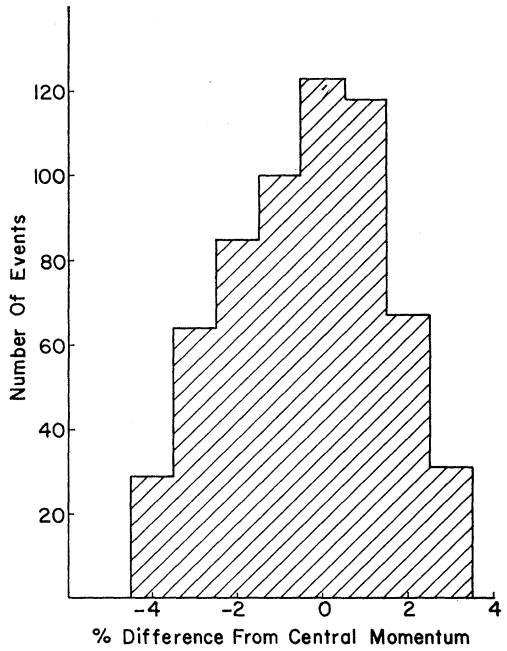

FIG. 2. Momentum distribution of particles at the end of the beam channel as generated by a Monte Carlo technique.

The beam telescope in this experiment is shown in Fig. 1 and consisted of six counters. The first counter C_0 was a Čerenkov counter located in the mass slit assembly. It consisted of a $\frac{1}{2}$-in.-thick by 1-in.-wide strip of Plexiglas blackened on the downstream surface and mounted at an angle of 40° to the beam line.

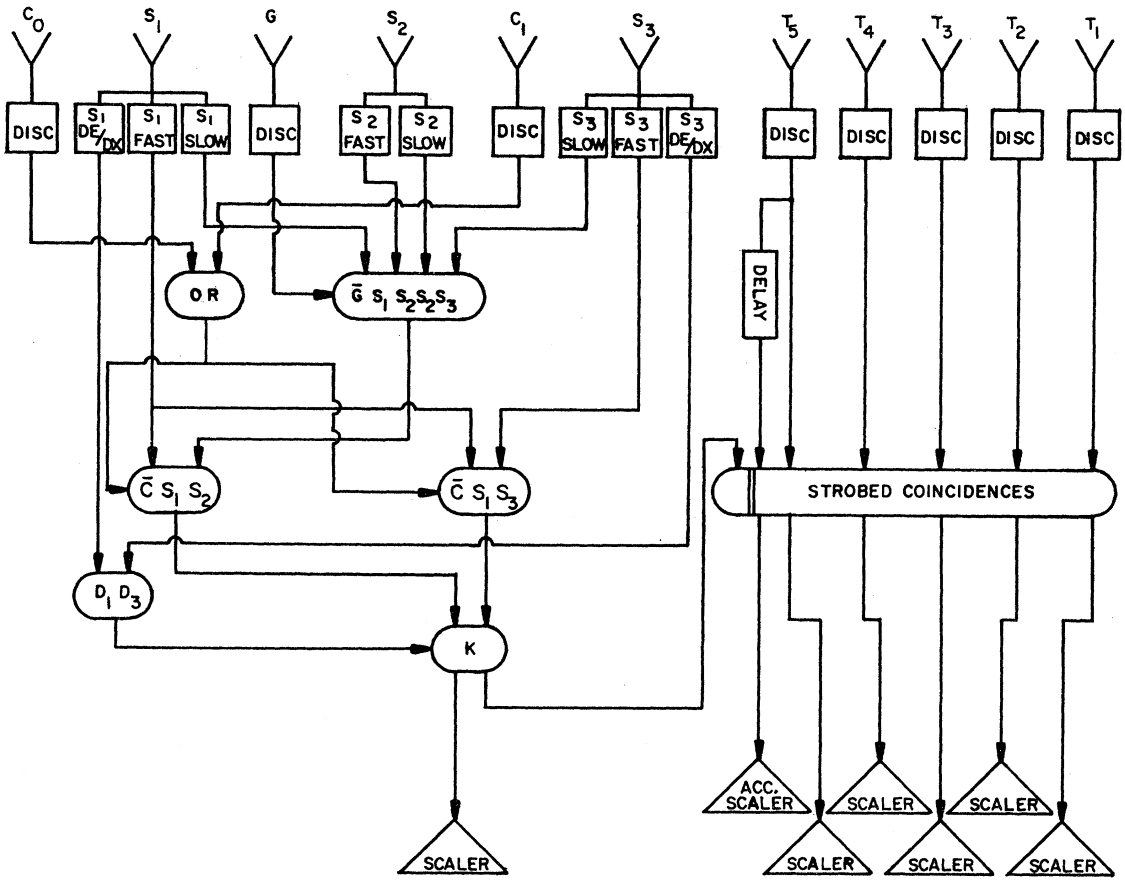

FIG. 3. Electronic logic diagram.

The other Čerenkov counter was a $\frac{7}{8}$-in.-thick piece of Plexiglas oriented perpendicular to the beam in a light-absorbing enclosure. It was viewed directly at each end by a photomultiplier tube. The critical angle for total internal reflection in this substance was about 42°, so that pions, muons, and electrons produced a signal from this counter at all momenta, whereas kaons passed undetected.

The first scintillation counter of the telescope, S_1, was located at the mass slit focus immediately downstream from C_0. This was combined in fast coincidence with S_2, a 3-in. by 6-in. scintillator with an isochronous light pipe, located just upstream from C_1. A similar fast coincidence was required between S_1 and S_3. The system was found to reject fast-particle beam contamination by a factor of 10^5.

Protons in the positive beam were rejected by the beam separator, by the S_1-S_2, S_1-S_3 time of flight, and by dE/dx, the doubles veto described below. The combined effect reduced proton contamination of the positive kaon signal to 1 part in 10^4.

The beam transmission was measured with a set of five scintillation counters T_1–T_5. These were mounted on a movable trolley so that the minimum detectable scattering angle could be altered with momentum to correspond to a constant value of four-momentum transfer, $|t| = 2.95 \times 10^{-3}$ $(\mathrm{GeV}/c)^2$. Transmission counter T_n had a radius of $7\sqrt{n}$ in. to bring the ratios of solid angles subtended to approximately integer values. S_4 was the last counter of the system and was located at the final focus of the beam. Its diameter was 5 in., and it was used to maintain a check on the efficiencies of the transmission counters.

Figure 3 is a diagram of the electronics. The three scintillation counters in the beam telescope each produced both a "FAST" and a "SLOW" signal. The FAST discriminator triggered at a low level and produced a very short output signal for timing, while the SLOW unit used a high level discrimination for noise rejection and a longer output. The S_3 SLOW discriminator was of the updating variety and the output signal of 50 nsec was clipped to 10 nsec. As a result the electronics was insensitive to any second beam particle which followed within 60 nsec of the first. This completely eliminated dead-time corrections to the transmission scaler readings. The output of $GS_1S_2S_2S_3$ preserved the timing information of the S_2 FAST signal, which was a 3-nsec signal timed to arrive at the coincidence unit several nanoseconds after the start of the other signals. The output was also very short and was used with the signal from S_1 FAST in

sharp coincidence for time-of-flight discrimination against protons. S_3 FAST and S_1 FAST were used in the same for further proton rejection. A pion signal in either of the Čerenkov counters vetoed these coincidences. The discrimination levels of S_1 (dE/dx) and S_3 (dE/dx) were set to trigger only on the largest 3% of the kaon pulses. A coincidence between these in the unit labeled D_1D_3 was used to veto simultaneous beam particles and to discriminate further against protons. An accidentals monitor signal was produced by delaying the T_5 signal one radio-frequency period of the Bevatron and combining this in coincidence with the undelayed kaon signal.

The efficiencies of the transmission counters were checked frequently by substituting a signal from S_4 for S_2 FAST, which was equivalent to requiring that a kaon pass through all five T counters.

III. DATA COLLECTION AND ANALYSIS

The techniques of transmission total-cross-section experiments have been well developed for other beam particles and other energies.[1–4,8,9] This experiment extended these methods to cover the special problems of a rapidly decaying beam at very low momentum.

Acquisition of Data

One of the major difficulties of an experiment with this type of beam is that the corrections, particularly for decaying particles, are extremely sensitive functions of the incident momentum. For this reason the momentum of the beam was measured twice during the experiment by finding its range in carbon. The measurements determine the average momentum of the beam to within ±0.5%.

During the run, the spatial distribution of the beam was measured immediately behind the target. This information was used to check the beam simulation program and to calculate the effective length of the target. The convergence of the beam through the target was found to have a negligible effect on this parameter.

The total-cross-section data were taken in three groups: First the K^+-nucleon cross sections were measured at 12 momentum settings. The experimental setup was then altered slightly to accommodate an associated 180° scattering experiment.[10] Several K^+ points were then remeasured to check consistency and to improve the statistics. Finally, the polarity of the beam was reversed and the K^--nucleon cross sections were measured.

The data taken at each momentum were divided into several short subruns, each of about ½ h duration. At the end of the subrun a different target flask was moved into position and a new subrun started. Data were thus taken on the targets sequentially and each was measured several times. In addition the efficiencies of the transmission counters were checked several times for each momentum point, typically after every third subrun. This technique checked the consistency of the raw data to about 0.05%.

In tuning the beam at each momentum, the timing of the S_1S_3 and S_1S_2 fast coincidences was set for maximum kaon flux. The fields of the separator were also set for maximum kaon flux except for some K^- points, where they were set for maximum K/π ratio.

Method of Analysis

The basic analysis was that of a standard good-geometry transmission experiment. If σ_i represents the cross section for scattering a beam particle out of counter i, and T_{ei} and T_{fi} are the transmissions as measured by this counter for empty and full targets, respectively, then

$$\sigma_i = (w/L\rho N_0)\ln(T_{ei}/T_{fi}) \quad (i=1,\ldots,5),$$

where w is the atomic weight of the target material, ρ is its density, L is its length, and N_0 is Avogadro's number. This expression contains no corrections for the difference between full- and empty-target decays which will be treated separately below. It should be noted that this expression includes scattering due to Coulomb effects which must then be calculated explicitly and subtracted to yield the nuclear scattering. These also will be discussed separately.

The transmissions were measured for a predetermined number of beam kaons, K, so that the standard deviation of a measured transmission is simply that of a binomial distribution,

$$\delta T = [T(1-T)/K]^{1/2}.$$

Thus the statistical error on σ_i is

$$\delta\sigma_i = \frac{w}{L\rho N_0}\left[\frac{(1-T_{ei})}{K_eT_{ei}} + \frac{(1-T_{fi})}{K_fT_{fi}}\right]^{1/2}.$$

Decay correction. Because the mean decay length of the kaon in this momentum range is short, and the probability of a decay product being counted is neither extremely high nor extremely low, a decay correction was needed which was much more precise that is usual in this type of experiment. This correction turned out to be about 6 mb for the highest points and increased to 30 mb for the lowest points. The method used was to perform three numerical integrations for each counter along the beam line from the beginning of the target to the counter in the following manner.

Let σ_i be the cross section for scattering a beam kaon out of counter i, and $N_i(x)$ be the number of kaons at

[8] A. Citrön, W. Galbraith, T. F. Kycia, B. A. Leontić, R. H. Phillips, A. Rousset, and P. H. Sharp, Phys. Rev. 144, 1101 (1966).

[9] D. V. Bugg, D. C. Salter, G. H. Stafford, R. F. George, K. F. Riley, and R. J. Tapper, Phys. Rev. 146, 980 (1966).

[10] P. K. Caldwell, T. Bowen, F. Ned Dikmen, E. W. Jenkins, R. M. Kalbach, D. V. Petersen, and A. E. Pifer, Phys. Rev. D 2, 1 (1970).

position x headed toward the counter. If $\sigma_{ei}(x)$ is an equivalent cross section for empty-target effects, then for the full and empty targets, respectively,

$$dN_{fi}=-N_{fi}(x)\left[\frac{\rho N_0}{w}[\sigma_i+\sigma_{ei}(x)]+\frac{m_k}{pc\tau_0}\right]dx$$

(inside the target)

$$=-N_{fi}(x)\left[\frac{\rho N_0}{w}\sigma_{ei}(x)+\frac{m_k}{pc\tau_0}\right]dx$$

(beyond the target)

and

$$dN_{ei}=-N_{ei}(x)\left[\frac{\rho N_0}{w}\sigma_{ei}(x)+\frac{m_k}{p_0c\tau_0}\right]dx,$$

where p_0 is the incident momentum, and p is the momentum at x. A straightforward integration and normalization yields

$$\frac{N_{fi}(D_i)}{N_f}=\exp\left[-\frac{L\rho N_0}{w}\sigma_i-\frac{\rho N_0}{w}\int_0^{D_i}\sigma_{ei}(x)dx-\int_0^{D_i}\frac{m_k}{pc\tau_0}dx\right]$$

and

$$\frac{N_{ei}(D_i)}{N_e}=\exp\left[-\frac{\rho N_0}{w}\int_0^{D_i}\sigma_{ei}(x)dx-\frac{m_kD_i}{p_0\tau c_0}\right],$$

where D_i is the counter position. Therefore,

$$\sigma_i=\frac{w}{L\rho N_0}\ln\left(\frac{N_{ei}(D_i)/N_e}{N_{fi}(D_i)/N_f}\right)+\frac{m_k}{c\tau_0}\int_0^{D_i}\left(\frac{1}{p}-\frac{1}{p_0}\right)dx.$$

Because the momentum loss in the target is not a simple function of x, it is necessary to integrate the second term numerically. Next it must be noted that the transmission T_i measured by the counter is not $N_i(D_i)/N$ since T_i also includes decay products which go forward and are counted:

$$T_i=[N_i(D_i)+N'(D_i)]/N.$$

$N'(D_i)$ is obtained by numerically integrating the expression

$$dN_i'=N_i(x)\frac{m_k}{pc\tau_0}P_i(x)dx,$$

where $N_i(x)$ is still the number of kaons headed toward the counter and $P_i(x)$ is a weighted average over all the decay modes of the probability that a product of a decay at x will be counted. Letting $T_i'=N_i'(D_i)/N$,

$$\sigma_i=\frac{w}{L\rho N_0}\ln\left(\frac{T_{ei}-T_{ei}'}{T_{fi}-T_{ei}'}\right)-\frac{m_k}{c\tau_0}\int_0^{D_i}\left(\frac{1}{p}-\frac{1}{p_0}\right)dx.$$

It should be noted that since dN_i' depends on N_i, it is a function of σ_i. Thus an iterative procedure is necessary to obtain a cross section. In practice, two iterations are generally sufficient to get cross sections that are self-consistent to within 0.01 mb. Also this correction takes into account double scattering by allowing small-angle scatterings to continue to be considered as part of the beam. Once a particle is scattered out of the counter, no allowance is made for the possibility of its decaying back into the counter. This effect is partially compensated by the overestimation of $P_i(x)$, which is calculated for a particle headed toward the center of the counter. Any errors in this procedure should be roughly proportional to the solid angle and should extrapolate to zero.

Coulomb corrections. There are three types of Coulomb effects inherent in any scattering experiment of this type. Of these, multiple scattering is the most difficult type to evaluate analytically. For this reason the experiment was designed to make this effect completely negligible. The smallest transmission counter was large enough to intercept beam particles scattered as much as approximately 5 standard deviations due to multiple scattering.

The other two effects, single Coulomb scattering and Coulomb-nuclear interference scattering, cannot be eliminated by experimental design and a correction must be made for each. The Coulomb corrections in this experiment were made by the method explained in Citrön *et al.*,[8] appropriately modified for the kaon-nucleon system. The limits, $t_{\max}$, of the step function approximation for the proton form factor were maintained at 0.12 F and 0.24 F for the direct Coulomb and interference integrals, respectively. These formulas were modified because of the lower velocity of the kaon beam:

$$\Delta\sigma_i(\text{direct Coulomb})=2\pi\hbar^2c^2\alpha^2\frac{1}{\beta^2}\left(\frac{1}{t_i}-\frac{1}{t_{\max}}\right)$$

and

$$\Delta\sigma_i(\text{interference})=4\pi\hbar c\alpha D\frac{1}{\beta p}\ln\left(\frac{t_{\max}}{t_i}\right),$$

where α is the fine-structure constant, β is the relative velocity, p is the c.m. momentum, and D is the real part of the forward scattering amplitude. The values of D used were obtained from the dispersion relation calculations of Zika,[11] and are listed in Table I.

Extrapolation. Once the σ_i's for nuclear scattering were obtained, a minimum χ^2 fit to the equation

$$\sigma_i=\sigma_T-\xi\Omega_i$$

was made, where Ω_i is the solid angle subtended by counter i, ξ is an adjustable parameter, and σ_T is the total cross section. It may easily be seen that the errors on the partial cross sections are strongly correlated,

[11] J. Zika, University of Arizona Physics Department (private communication).

TABLE I. Real parts of forward scattering amplitudes (see Ref. 11).

P_{lab} (MeV/c)	$D_{(K^+p)}$ (F)	$D_{(K^+n)}$ (F)	$D_{(K^-p)}$ (F)	$D_{(K^-n)}$ (F)
717	−0.30	−0.07	+0.17	+0.17
686	−0.30	−0.07	+0.14	+0.14
657	−0.30	−0.07	+0.11	+0.11
627	−0.30	−0.07	+0.07	+0.07
596	−0.30	−0.07	+0.02	+0.02
566	−0.30	−0.07	−0.04	−0.04
536	−0.30	−0.07	−0.06	−0.06
506	−0.30	−0.07	−0.09	−0.09
475	−0.30	−0.07	−0.14	−0.14
440	−0.30	−0.07	−0.18	−0.18
405	−0.30	−0.07	−0.14	−0.14
385	−0.30	−0.07	−0.06	−0.06
366	−0.30	−0.07	+0.04	+0.04

TABLE II. K^+p and K^+d total cross sections.

P_{lab} (MeV/c)	σ_{K^+p} (mb)	Increased error	σ_{K^+d} (mb)	Increased error
717	11.14±0.25	0.50	26.02±0.24	0.41
686	11.40±0.18	0.40	25.68±0.14	0.36
657	12.20±0.20	0.63	26.03±0.17	0.33
627	12.33±0.14	0.39	26.15±0.17	0.40
596	12.94±0.19	0.34	25.40±0.16	0.20
566	13.05±0.19	0.25	25.17±0.16	0.18
536	12.35±0.20	0.57	24.11±0.17	0.49
506	12.99±0.23	0.28	23.77±0.19	0.19
475	13.44±0.17	0.29	23.29±0.16	0.20
440	12.97±0.23	0.51	22.31±0.20	0.36
405	13.55±0.31	0.48	21.61±0.26	0.32
366	13.28±0.35	0.64	20.74±0.30	0.48

since the counters overlap. A statistical analysis of the experimental geometry gives an error matrix M_{ij} of σ_i and σ_j in the form

$$M_{ij}=(\delta\sigma_j)^2 \quad (j\geq i).$$

Since M is symmetric, this defines the entire matrix. χ^2 is then of the form

$$\chi^2=\sum_{ij}(\sigma_T-\xi\Omega_i-\sigma_i)(M^{-1})_{ij}(\sigma_T-\xi\Omega_j-\sigma_j).$$

The minimization condition defines a transformation matrix T, which maps the five-dimensional space containing the σ_i's onto the two-dimensional space containing σ_T and ξ. This transformation applied to M yields the errors on σ_T and ξ. A typical set of σ_i's and the fitted line are shown in Fig. 4.

Unfolding and separation of isospin states. In each data point there was a large momentum spread caused by energy loss in the target, necessitating a momentum-unfolding procedure for the proton as well as the deuteron data. The proton version used a momentum distribution obtained for each point by folding together the incident-beam momentum spread and the losses in the target. The deuteron version used the Fermi momentum distribution as determined from the Moravscik deuteron wave function,[12] as well as the spread of the beam momentum.

The pure $I=0$ and $I=1$ isospin states were extracted from the unfolded cross-section curves with the aid of the formula for the deuteron cross section,

$$\sigma_d=\sigma_p+\sigma_n-\sigma_g.$$

σ_g is the Glauber screening correction[1–4] as modified by

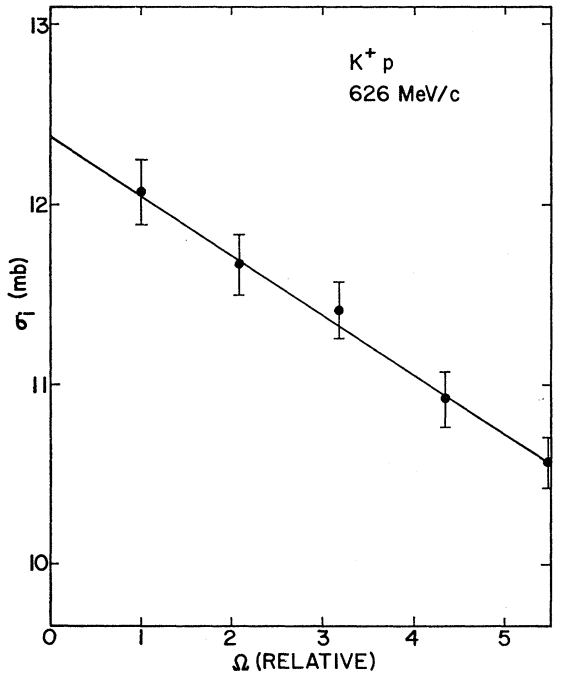

FIG. 4. Typical set of partial cross sections and the fitted line used to extract the cross section at zero solid angle.

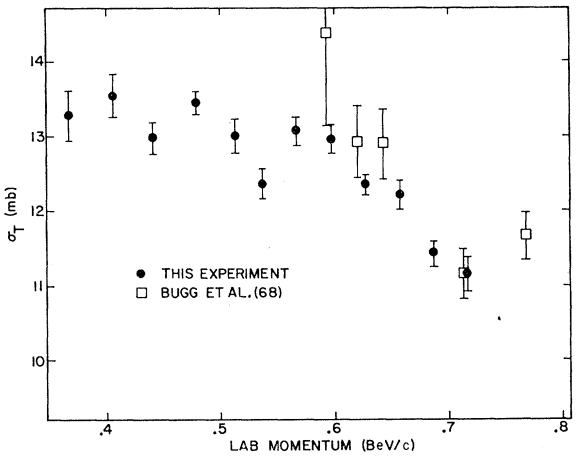

FIG. 5. K^+p total cross sections before correction for beam momentum distribution.

[12] G. Lynch, LRL Physics Notes, Memo No. 600, 1966 (unpublished).

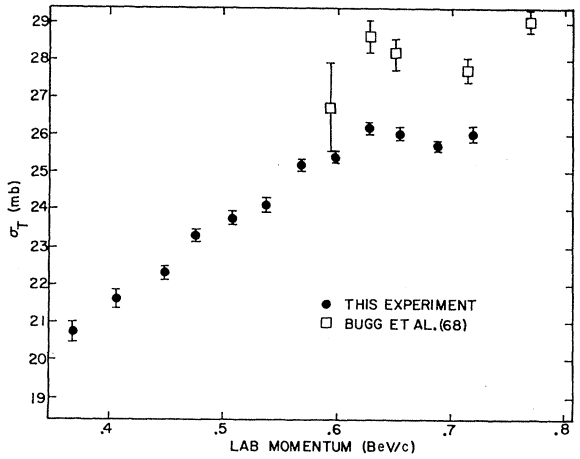

FIG. 6. K^+d total cross sections before correction for beam and Fermi momentum distributions.

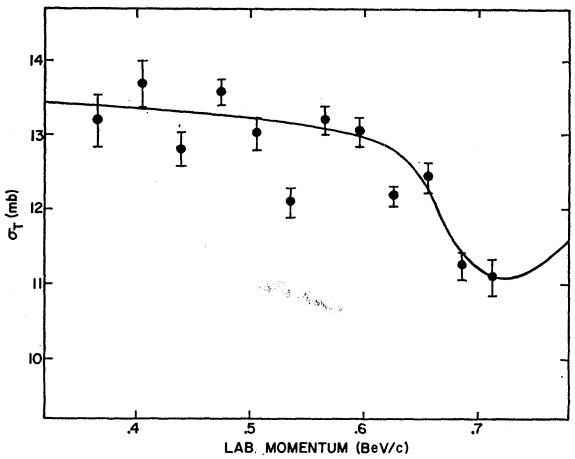

FIG. 7. Corrected K^+p total cross sections. Curve is a suggested fit to the data, taking into account data outside the range of this experiment.

Wilkin[13]:

$$\sigma_g = \frac{\langle r^{-2}\rangle}{4\pi}[2\sigma_p\sigma_n(1-\rho_p\rho_n) - \tfrac{1}{2}\sigma_p^2(1-\rho_p^2) - \tfrac{1}{2}\sigma_n^2(1-\rho_n^2)].$$

The factor $\langle r^{-2}\rangle$, for the deuteron wave function, was taken to be 0.3 F^{-2}. The factors ρ_p and ρ_n are the ratios of the real to the imaginary parts of the forward scattering amplitude for kaons on protons and neutrons, respectively. If σ_0 represents the pure $I=0$ cross section and σ_1 the pure $I=1$ cross section, then for the K^+-nucleon system $\sigma_1=\sigma_p$ and $\sigma_0=2\sigma_n-\sigma_p$, and for the K^--nucleon system $\sigma_1=\sigma_n$ and $\sigma_0=2\sigma_p-\sigma_n$.

IV. RESULTS AND CONCLUSIONS

K^+-Nucleon Data

The measured total cross sections for K^+p and K^+d are listed in Table II, and are shown in Figs. 5 and 6, respectively, with the recent results of the experiment by Bugg *et al.*[4] The error bars shown are from counting statistics only. The Table II columns "increased errors" appear because statistical analysis of the data showed a discrepancy between subruns on each target that could not be accounted for by counting statistics alone and which appear to have been random in time. In order to include this as additional statistical error as much as possible, χ^2 was computed for the set of n measurements of a transmission under the hypothesis of a constant transmission. If counting statistics alone contribute to the error, χ^2 should be approximately equal to $n-1$. Thus $[\chi^2/(n-1)]^{1/2}$ was taken as a measure of the factor by which the statistical error of the measurement of that transmission should be increased. The increased errors on the full- and empty-target transmissions were combined in the same way as the statistical errors to obtain an increased error $(\delta\sigma_i)_{\text{inc}}$ on the partial cross section σ_i. Finally, an

TABLE III. K^+N momentum-unfolded cross sections.

P_{lab} (MeV/c)	σ_{K^+p} (mb)	σ_{K^+d} (mb)	σ_1 (mb)	σ_0 (mb)
717	11.10±0.25	25.13±0.41	11.10±0.25	17.79±1.11
686	11.25±0.18	24.68±0.36	11.25±0.18	16.43±0.90
657	12.43±0.20	26.76±0.33	12.43±0.20	17.20±0.89
627	12.18±0.14	27.60±0.30	12.18±0.14	19.66±0.73
596	13.04±0.19	26.37±0.28	13.04±0.19	14.60±0.80
566	13.20±0.19	25.49±0.26	13.20±0.19	12.32±0.77
536	12.09±0.20	24.70±0.24	12.09±0.20	14.03±0.77
506	13.02±0.23	24.16±0.23	13.02±0.23	10.14±0.83
475	13.58±0.17	24.28±0.23	13.58±0.17	8.71±0.69
440	12.81±0.23	23.46±0.24	12.81±0.23	9.37±0.84
405	13.69±0.31	21.97±0.26	13.69±0.31	3.61±1.07
366	13.20±0.35	21.41±0.30	13.20±0.35	3.99±1.21

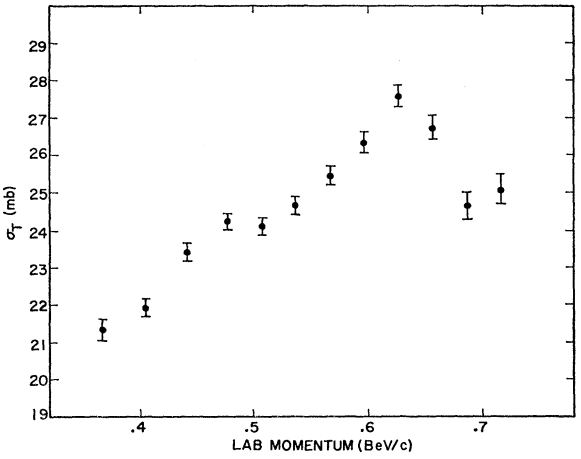

FIG. 8. Corrected K^+d total cross sections.

[13] C. Wilkin, Phys. Rev. Letters 17, 561 (1966).

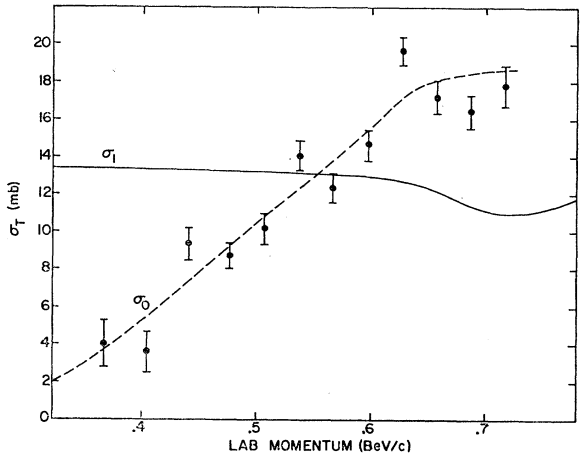

FIG. 9. K^+N, $I=0$ (σ_0) total cross sections. Curves are explained in the text.

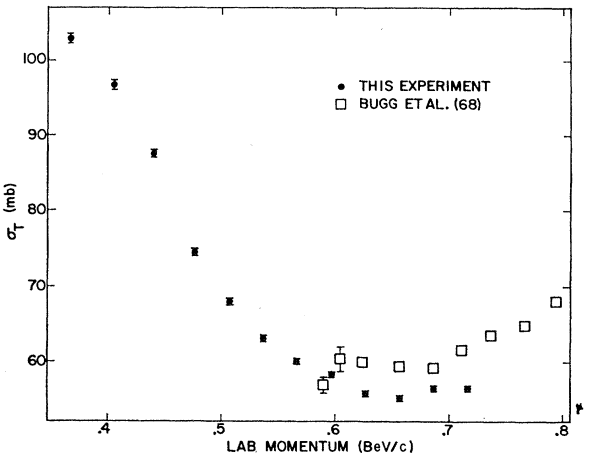

FIG. 11. K^-d total cross sections before correction for beam and Fermi momentum distributions.

over-all increase factor was computed:

$$F=\tfrac{1}{5}\sum_{i=1}^{5}\frac{(\delta\sigma_i)_{\text{inc}}}{(\delta\sigma_i)_{\text{stat}}}.$$

The statistical error on the extrapolation, determined by the set of $(\delta\sigma_i)_{\text{stat}}$, was multiplied by F and the result entered under "increased error."

The result of correcting the proton data for the effect of the beam momentum spread is presented in Fig. 7 and is listed in Table III. It was found that the experimental data could not be fitted to an effective-range formula of the form

$$\sigma_T=\frac{4\pi a^2}{1+a(a+r)k^2+\frac{1}{4}a^2r^2k^4}+\frac{4\pi b^2k^4}{1+b^2k^6},$$

where a and b are the S- and P-wave scattering lengths, respectively, r is the effective range, and $k=p/\hbar$ is the wave number. It may be noticed that there is a significant systematic disagreement between the K^+d data of this experiment and those of Bugg *et al.*, while the hydrogen data agree quite well. This same disagreement appears in the K^-d data. This suggests a fundamental difficulty in the treatment of the deuterium data in one of the experiments, but at the present time we cannot account for the disagreement.

The deuterium data corrected for the effects of both the beam and Fermi momentum distributions appear in Fig. 8 and in Table III. Since the unfolding process results in strong correlations, the errors on the unfolded cross sections were estimated using a Monte Carlo technique. The $I=0$ (σ_0) cross sections obtained are shown in Fig. 9 and in Table III. The σ_1 curve from Fig. 7 is added for comparison. The σ_0 data points result from combining the corrected proton and deuteron data points with the Glauber-Wilkin correction; the dashed σ_0 curve is simply a suggested smooth curve.

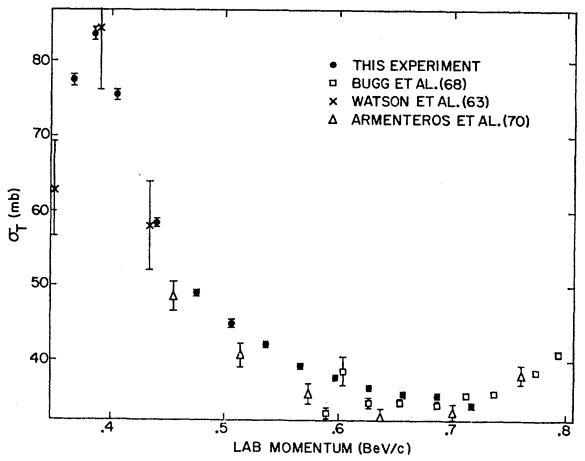

FIG. 10. K^-p total cross sections before correction for beam momentum distribution.

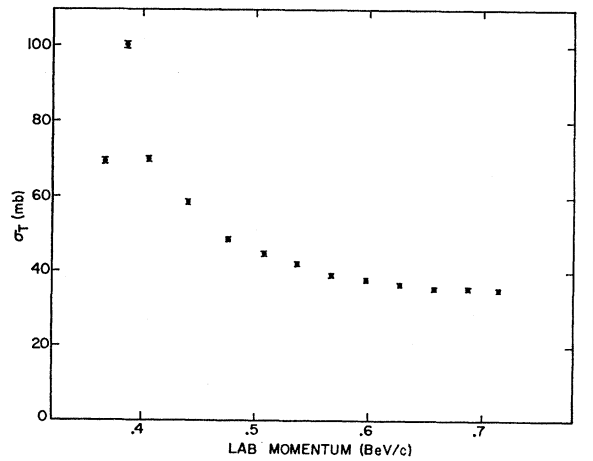

FIG. 12. Corrected K^-p total cross sections.

TABLE IV. K^-p and K^-d total cross sections.

P_{lab} (MeV/c)	σ_{K^-p} (mb)	Increased error	σ_{K^-d} (mb)	Increased error
717	34.01±0.37	0.38	56.50±0.34	0.35
686	35.29±0.39	0.42	56.45±0.34	0.46
657	35.53±0.33	0.33	55.22±0.32	0.44
627	36.41±0.28	0.37	55.80±0.26	0.26
596	37.76±0.33	1.16	58.34±0.29	0.96
566	39.29±0.34	0.39	60.04±0.29	0.73
536	42.08±0.38	0.38	63.07±0.33	0.38
506	44.94±0.45	0.57	67.93±0.39	0.46
475	48.96±0.47	0.56	74.53±0.42	0.49
440	58.42±0.57	1.16	87.57±0.50	0.92
405	75.54±0.68	0.71	96.74±0.64	0.64
385	83.75±0.83	0.87	···	···
366	77.24±0.79	1.04	102.93±0.70	1.02

Although there is a possibility of an enhancement at 630 MeV/c, the data are consistent with there being no structure at all. A resonance in this region would have to be highly elastic because it is just above inelastic threshold (520 MeV/c) and the inelastic cross section in this region is very small. This implies that it would have a height on the order of $4\pi/k^2$, about 37 mb. The absence of any such resonance in this region is evident.

K^--Nucleon Data

Table IV gives the K^-p and K^-d measured total cross sections, which are presented with the data of Bugg *et al.*,[4] Watson *et al.*,[6] and Armenteros *et al.*[7] in Figs. 10 and 11. The cross sections of the proton and deuteron, corrected for the beam and Fermi momentum distributions, are shown in Figs. 12 and 13, respectively, and listed in Table V. The prominence of the structure near 400 MeV/c is clearly confirmed.

Inelastic channels are open to the K^--nucleon system at all energies in both isospin states. Thus S-wave effective-range theory indicates that the background total cross section for low momentum should have the form

$$\sigma_b = c_1/p + c_2 + c_3 p.$$

The $I=1$ cross sections appear in Fig. 14 and Table V and are consistent with such a rise at very low momenta.

TABLE V. K^-N momentum-unfolded cross sections.

P_{lab} (MeV/c)	σ_{K^-p} (mb)	σ_{K^-d} (mb)	σ_0 (mb)	σ_1 (mb)
686	35.33±0.39	54.40±0.79	50.3±1.4	20.33±0.88
657	35.40±0.33	50.52±0.74	54.9±1.2	15.87±0.81
627	36.36±0.28	51.58±0.68	56.7±1.1	16.07±0.74
596	37.80±0.33	55.12±0.64	57.1±1.2	18.55±0.72
566	39.10±0.34	56.40±0.62	59.7±1.2	18.50±0.70
536	42.15±0.38	55.87±0.62	70.1±1.3	14.16±0.73
506	44.71±0.45	57.46±0.63	76.7±1.5	12.75±0.77
475	48.45±0.47	64.08±0.65	81.1±1.6	15.84±0.80
440	58.41±0.57	78.64±0.68	96.0±1.8	20.77±0.89
405	69.80±0.68	92.47±0.70	116.0±2.2	23.59±0.98
385	100.19±0.83	···	174.4±2.8	···
366	69.32±0.79	95.01±0.73	110.3±2.5	28.31±1.08

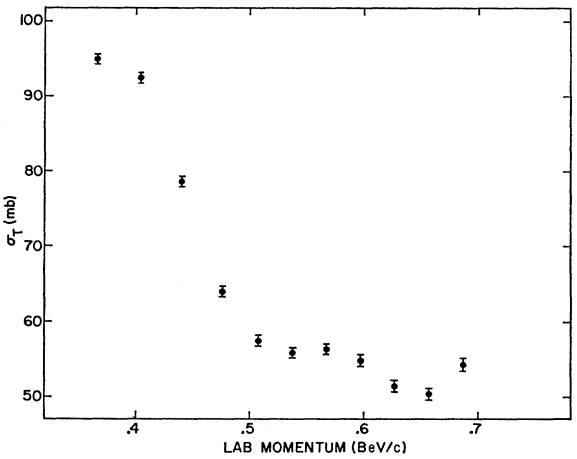

FIG. 13. Corrected K^-d total cross sections.

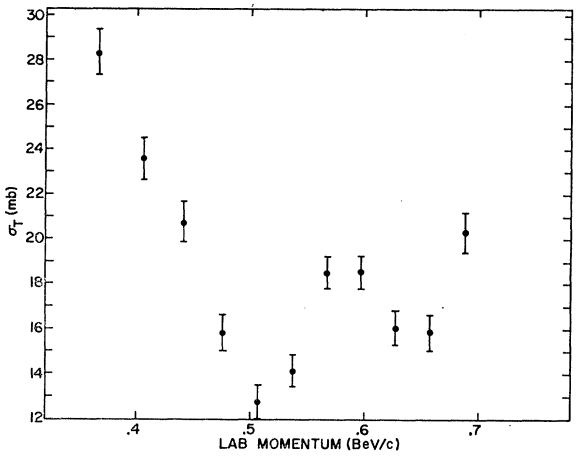

FIG. 14. K^-N, $I=1$ total cross sections.

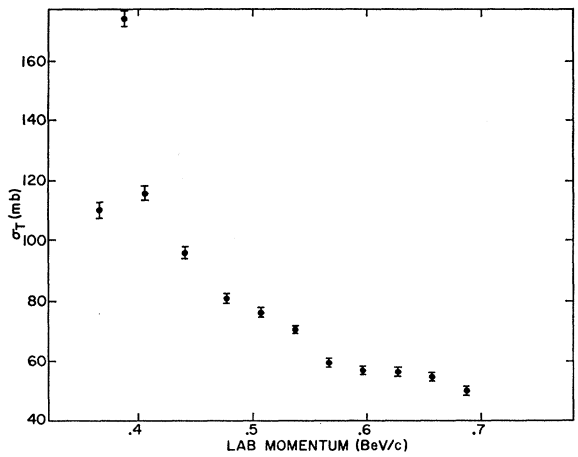

FIG. 15. K^-N, $I=0$ total cross sections.

There is a strong suggestion of structure at 580 MeV/c, which corresponds to a mass of 1600 MeV. The increase at the upper end of our range is due to the influence of

the well-known resonances $\Sigma(1670)$ and $\Sigma(1765)$ at 740 and 940 MeV/c, respectively.

The $I=0$ points are presented in Fig. 15. They were fitted assuming the background given above and a Breit-Wigner form for the $\Lambda'(1520)$, with subtraction of Breit-Wigner tails of well-known higher-mass resonances. A best fit to this data was achieved with a width of $\Gamma=6\pm1$ MeV and an elasticity of 0.60 ± 0.05 for the $\Lambda'(1520)$ at a mass of 1518 MeV. This compares to a previously published width of 16 MeV.[14] This disagreement may be indicative of the difficulties that arise with the unfolding procedure when the width of structure encountered is of the same order as the separation of the experimental points.

Systematic Errors

The systematic errors due to uncertainty in the correction for Coulomb effects arose almost entirely from an uncertainty in the real parts of the forward scattering amplitudes. The real parts of the K^+p amplitudes are believed correct to within 0.02 F, which implies a 0.7% error in the K^+p cross section, while the K^+n should be correct to within 0.01 F. This leads to an uncertainty of 0.6% in the K^+d total cross sections. While the percentage error in the real part of the K^-p scattering amplitude is much larger, it is much less important in the cross section because of the large imaginary part of the scattering amplitude, and so an error of 0.1% is expected in σ_T for K^-p. The K^-n forward scattering amplitude is the least well known of all, and an error of 0.3% in the K^-d total cross sections from this source would not be surprising.

Further systematic errors arise from uncertainty in the target density. For the hydrogen this produces an uncertainty of 0.2% and for deuterium, 0.5%. Also the effective length of the target is uncertain by 0.1%. However, the spread of solid angles due to the finite target is believed to contribute negligible error since the average solid angles were determined by a numerical integration over the beam shape and target volume, and since only the ratio of the solid angles was used.

Summary

Perhaps the most significant results of this experiment were (a) the establishment of the dip in the K^+p cross section around 700 MeV/c and its reflection in the K^+d cross section, and (b) the indication of a possible resonance in the K^-N, $I=1$ cross section at about 580 MeV/c. The demonstration that in the K^+N, $I=1$ cross section the effective range, even with a P wave added, is not an adequate parametrization in this energy region is interesting. The dramatic nature of the $\Lambda'(1520)$ in the K^-N, $I=0$ cross section is similarly interesting, but probably not so much as the lack of further structure in this momentum range.

ACKNOWLEDGMENTS

We wish to acknowledge the members of the Bevatron staff and crew, in particular, W. Hartsough, for their cooperation. We also wish to thank T. Elioff for his advice and encouragement during the experiment.

[14] A. Barbaro-Galtieri, S. E. Derenzo, L. R. Price, A. Rittenberg, A. H. Rosenfeld, N. Barash-Schmidt, C. Bricman, M. Roos, P. Söding, and C. G. Wohl, Rev. Mod. Phys. **42**, 87 (1970).